Constant-temperature molecular dynamics with momentum conservation

K. Cho and J. D. Joannopoulos
Department of Physics, Massachusetts Instutite of Technology, Cambridge, Massachusetts 02139

Leonard Kleinman
Department of Physics, University of Texas, Austin, Texas 78712
(Received 28 September 1992)

The Nosé theorem of the extended-system method of the constant-temperature molecular dynamics is generalized by including the conservation of the total virtual momentum. It is proved that a canonical ensemble of an $(N-1)$-particle system is generated from an extended system of an N-particle system *only* if the total virtual momentum is zero. It is also shown that the resulting $(N-1)$-particle system has a slightly different mass spectrum than that of the original N-particle system. The consequences of this new mass spectrum are relevant in the calculation of dynamical properties and the relaxation times of the system, but irrelevant to thermodynamic averages. For practical considerations, numerical simulations are performed and tested against this theorem. The differences in application of the Nosé theorem and the generalized Nosé theorem are discussed.

PACS number(s): 05.20.Gg, 02.70.Ns, 02.60.Cb

I. INTRODUCTION

Molecular dynamics (MD) is a computational method that numerically solves Newton's equations of motion by performing a discrete-time integration [1]. According to the assumption of ergodicity, one can generate an ensemble by collecting the physical states at each discrete time step. The ensemble generated by the MD method depends on the boundary conditions [2]. For particles *in a box* the ensemble generated is the traditional microcanonical ensemble where only the total energy of the system is conserved. For periodic boundary conditions (which are preferred in simulations) the ensemble is no longer strictly microcanonical because in this case the total linear momentum is also conserved [3].

In some cases, the neglect of the conservation of the total momentum will introduce only a small amount of error in the interpretation of MD simulation results [1]. However, there are cases where the conservation of the total momentum should play a crucial role in determining the nature of an ensemble generated by the MD method. We have discovered that the extended-system method of Nosé is precisely such a case.

The extended-system method (ESM) introduces an extra dynamical variable to simulate the effect of the heat reservoir or the pressure reservoir [4–6]. The ESM of the constant-temperature molecular dynamics is known to generate a canonical ensemble of a physical system if the extended system (ES) is ergodic [6–9]. This generation of a canonical ensemble from an ergodic ES is guaranteed by the Nosé theorem within the Hamiltonian formalism [6]. However, in this theorem, only the conservation of the total ES energy is used, and the conservation of the total virtual momentum and the total virtual angular momentum are ignored [6].

One can safely ignore the conservation of the total virtual *angular* momentum because it is not conserved during the simulation if a periodic boundary condition is used [2]. However, one cannot ignore the conservation of the total virtual momentum because this *is* conserved during numerical simulations. Therefore the Nosé theorem is no longer strictly valid for actual ESM simulations. Consequently, any theoretical proof which will determine the conditions under which one can obtain the canonical ensemble of a physical system from the ESM must include the conservation of the total virtual momentum as well as the conservation of the total ES energy.

In this paper, we generalize the Nosé theorem by including the conservation of the total virtual momentum and prove analytically that a canonical ensemble is generated from the ES *only if* the total virtual momentum is *zero*. This generalized Nosé theorem shows that the physical system satisfying a canonical ensemble is an $(N-1)$-particle system with a different mass spectrum from that of the original N-particle physical system.

We also perform simulations with zero and nonzero total virtual momentum in order to demonstrate, in a practical way, the consequences of the generalized Nosé theorem. Finally, we discuss the practical considerations related to the difference of these two theorems.

This paper is organized as follows. In Sec. II we prove the generalized Nosé theorem. In Sec. III we study the effect of nonzero total virtual momentum using numerical simulations. In Sec. IV we discuss the practical considerations related to the generalized Nosé theorem. In Sec. V we summarize and conclude.

II. GENERALIZED NOSÉ THEOREM

In this section, we prove the generalized Nosé theorem by calculating the ES partition function with both the energy conservation and the total virtual momentum conservation which are the valid conditions for practical applications. The following is the generalized Nosé

theorem: if ES is *ergodic* and if the total linear virtual momentum of the N-particle physical system is *zero*, then the ESM will generate a canonical ensemble for an $(N-1)$-particle system with a *different* mass spectrum.

For the proof, we assume the ergodicity of the ES so that the ES partition function has a microcanonical ensemble form of energy δ function and momentum δ function. The partition function of an ergodic ES is

$$Z=c\int\prod_{i=1}^{N}d\mathbf{r}_i d\mathbf{p}_i\int ds\,dP_s\,\delta(H_{\rm ES}-E)\delta\left[\sum_{i=1}^{N}\mathbf{p}_i-\mathbf{P}_0\right], \tag{2.1}$$

where the ES Hamiltonian is expressed in terms of its own canonical variables as follows [10]:

$$H_{\rm ES}(\mathbf{r}_i,\mathbf{p}_i,s,P_s)=\sum_{i=1}^{N}\frac{\mathbf{p}_i^2}{2m_i s^2}+\phi(\{\mathbf{r}_i\})+\frac{P_s^2}{2Q}+gk_B T_{\rm ext}\ln(s)\ . \tag{2.2}$$

By introducing the center-of-mass (c.m.) momenta, $\tilde{\mathbf{p}}_i=\mathbf{p}_i-\mathbf{P}_0/N$, the kinetic-energy term becomes a sum of the relative kinetic energy and the c.m. kinetic energy as follows:

$$\sum_{i=1}^{N}\frac{\mathbf{p}_i^2}{2m_i s^2}=\sum_{i=1}^{N}\frac{\tilde{\mathbf{p}}_i^2}{2m_i s^2}+\frac{\mathbf{P}_0^2}{2Ms^2}\ , \tag{2.3}$$

where $M=\sum_{i=1}^{N}m_i$. The partition function can be expressed using the c.m. momenta as follows:

$$Z=c\int\prod_{i=1}^{N}d\mathbf{r}_i d\tilde{\mathbf{p}}_i\int ds\,dP_s\,\delta(H_{\rm ES}-E)\delta\left[\sum_{i=1}^{N}\tilde{\mathbf{p}}_i\right], \tag{2.4}$$

where $H_{\rm ES}$ is

$$H_{\rm ES}=\sum_{i=1}^{N}\frac{\tilde{\mathbf{p}}_i^2}{2m_i s^2}+\frac{\mathbf{P}_0^2}{2Ms^2}+\phi(\{\mathbf{r}_i\})+\frac{P_s^2}{2Q}+gk_B T_{\rm ext}\ln(s)\ . \tag{2.5}$$

Now, one can eliminate the momentum δ function by performing an integration of $\tilde{\mathbf{p}}_N$ and obtain

$$Z=c\int\prod_{i=1}^{N}d\mathbf{r}_i\prod_{i=1}^{N-1}d\tilde{\mathbf{p}}_i\int ds\,dP_s\,\delta(H_{\rm ES}-E)\ , \tag{2.6}$$

where the argument of the energy δ function, $H_{\rm ES}-E$, is

$$H_{\rm ES}-E=\sum_{i=1}^{N-1}\frac{\tilde{\mathbf{p}}_i^2}{2m_i s^2}+\frac{\left[\sum_{i=1}^{N-1}\tilde{\mathbf{p}}_i\right]^2}{2m_N s^2}+\frac{\mathbf{P}_0^2}{2Ms^2}+\phi(\{\mathbf{r}_i\})+\frac{P_s^2}{2Q}+gk_B T_{\rm ext}\ln(s)-E\ . \tag{2.7}$$

The next step is to diagonalize the inverse mass matrix M^{-1}, where

$$(M^{-1})_{ij}=\frac{1}{m_N}+\frac{1}{m_i}\delta_{ij}\ . \tag{2.8}$$

This can be done easily by introducing normal-mode momenta π_i such that

$$\sum_{i=1}^{N-1}\frac{\tilde{\mathbf{p}}_i^2}{2m_i s^2}+\frac{\left[\sum_{i=1}^{N-1}\tilde{\mathbf{p}}_i\right]^2}{2m_N s^2}=\sum_{i=1}^{N-1}\frac{\pi_i^2}{2\lambda_i s^2}\ . \tag{2.9}$$

If the masses are identical (i.e., $m_i=m$), one then obtains $\lambda_i=m$ for $i=1,\ldots,N-2$ and $\lambda_{N-1}=m/N$. After this diagonalization, the partition function becomes

$$Z=c\int\prod_{i=1}^{N}d\mathbf{r}_i\prod_{i=1}^{N-1}d\pi_i\int ds\,dP_s\,\delta\left[\sum_{i=1}^{N-1}\frac{\pi_i^2}{2\lambda_i s^2}+\frac{\mathbf{P}_0^2}{2Ms^2}+\phi(\{\mathbf{r}_i\})+\frac{P_s^2}{2Q}+gk_B T_{\rm ext}\ln(s)-E\right]. \tag{2.10}$$

Finally, one introduces the physical momenta, $\mathbf{p}_i'=\pi_i/s$, to eliminate the s variable in the kinetic-energy term and obtains the partition function as follows:

$$Z=c\int\prod_{i=1}^{N}d\mathbf{r}_i\prod_{i=1}^{N-1}d\mathbf{p}_i'\int ds\,dP_s\,s^{3N-3}\delta\left[\sum_{i=1}^{N-1}\frac{\mathbf{p}_i'^2}{2\lambda_i}+\frac{\mathbf{P}_0^2}{2Ms^2}+\phi(\{\mathbf{r}_i\})+\frac{P_s^2}{2Q}+gk_B T_{\rm ext}\ln(s)-E\right]. \tag{2.11}$$

This integral has a similar form to the one in the original formulation of Nosé except for the presence of the c.m. kinetic-energy term in the energy δ function and $3N-3$ momentum integration instead of $3N$. In the following, we perform the s integration, and discuss the consequences of the differences between the integral (2.11) and the original integral of Nosé [6].

In general, if $\mathbf{P}_0\neq\mathbf{0}$, the argument of the energy δ function has two roots of s, s_1, and s_2, as illustrated in Fig. 1, and the δ function becomes as follows:

$$\sum_{i=1}^{2}\frac{\delta(s-s_i)}{|-K_0/s^3+gk_B T_{\rm ext}/s|_{s=s_i}}\ , \tag{2.12}$$

where $K_0=\mathbf{P}_0^2/2M$. The integration over s gives the following expression:

$$Z=c\int\prod_{i=1}^{N}d\mathbf{r}_i\prod_{i=1}^{N-1}d\mathbf{p}_i'\int ds\,dP_s s^{3N-3}\sum_{i=1}^{2}\frac{\delta(s-s_i)}{|-K_0/s^3+gk_BT_{\rm ext}/s|_{s=s_i}}$$
$$=c\int\prod_{i=1}^{N}d\mathbf{r}_i\prod_{i=1}^{N-1}d\mathbf{p}_i'\int dP_s\sum_{i=1}^{2}\frac{s_i^{3N-3}}{|-K_0/s^3+gk_BT_{\rm ext}/s|_{s=s_i}}\ . \tag{2.13}$$

Obviously, the integrand is not the Boltzmann factor of a physical Hamiltonian.

In the case of $\mathbf{P}_0=\mathbf{0}$, the problem simplifies considerably, and one can perform the integration over s in (2.1) immediately. For completeness, however, we use (2.13) and set $K_0=0$. Since $\mathbf{P}_0=\mathbf{0}$, there is only one root of s, s_0, as shown in Fig. 1, and one obtains

$$Z=c\int\prod_{i=1}^{N}d\mathbf{r}_i\prod_{i=1}^{N-1}d\mathbf{p}_i'\int dP_s s_0^{3N-3}\frac{s_0}{gk_BT_{\rm ext}}$$
$$=c'\int\prod_{i=1}^{N}d\mathbf{r}_i\prod_{i=1}^{N-1}d\mathbf{p}_i'e^{-\beta_{\rm ext}H_0}\int dP_s e^{-\beta_{\rm ext}P_s^2/2Q}\ , \tag{2.14}$$

where $g=3N-2$ is used, and H_0 is the physical Hamiltonian,

$$H_0=\sum_{i=1}^{N-1}\frac{\mathbf{p}_i'^2}{2\lambda_i}+\phi(\{\mathbf{r}_i\})\ . \tag{2.15}$$

Therefore one obtains a canonical ensemble of the $(N-1)$-particle system with the mass spectrum $\{\lambda_i\}$ from the N-particle system with the mass spectrum $\{m_i\}$ only if total virtual momentum is zero. This completes the proof of the generalized Nosé theorem [11].

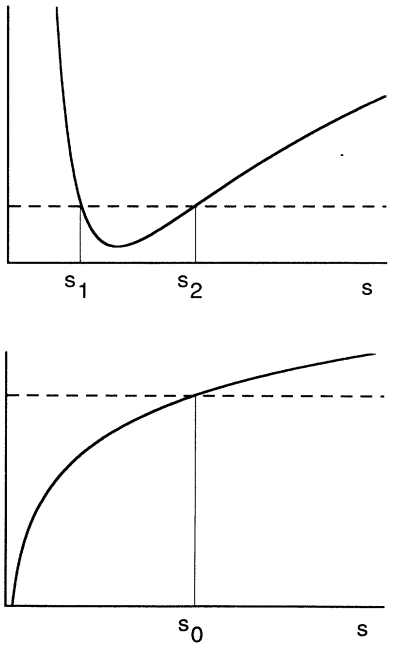

FIG. 1. Top panel illustrates two solutions of the equation $K_0/s^2+gk_BT_{\rm ext}\ln(s)=E_0$ with $K_0\neq0$. Bottom panel illustrates the solution of the equation with $K_0=0$.

III. NUMERICAL SIMULATIONS

In this section we perform numerical simulations of the extended Lennard-Jones (LJ) system with both zero and nonzero total virtual momentum, and test the simulations against the generalized Nosé theorem. In Sec. III A we derive the analytic expression for the average moments of the instantaneous temperature and the thermostat kinetic energy from the canonical ensemble. In Sec. III B we compare these quantities with the results of numerical simulations.

A. Analytic expression of moments

In this section we describe the canonical-ensemble expression of the moments of the instantaneous temperature of the LJ system and the thermostat kinetic energy. The instantaneous temperature T is defined as follows:

$$T=\frac{2}{(3N-3)k_B}K\ , \tag{3.1}$$

where K is the kinetic energy of $N-1$ particles. The analytic expressions of the moments of the instantaneous temperature fluctuation are obtained from a canonical ensemble as follows:

$$\langle T\rangle=T_{\rm ext}\ , \tag{3.2}$$
$$\langle T^2\rangle_c=\frac{2}{f}T_{\rm ext}^2\ , \tag{3.3}$$
$$\langle T^3\rangle_c=\frac{8}{f^2}T_{\rm ext}^3\ , \tag{3.4}$$
$$\langle T^4\rangle_c=\left[\frac{2}{f}\right]^3\left[\frac{3f}{2}+6\right]T_{\rm ext}^4\ , \tag{3.5}$$

where $f=3N-3$, $\langle\ \rangle$ represents an ensemble average, and $\langle T^m\rangle_c=\langle(T-\langle T\rangle)^m\rangle$.

The moments of thermostat kinetic energy are the following:

$$\langle K_s\rangle=\tfrac{1}{2}k_BT_{\rm ext}\ , \tag{3.6}$$
$$\langle K_s^2\rangle_c=\tfrac{1}{2}(k_BT_{\rm ext})^2\ , \tag{3.7}$$
$$\langle K_s^3\rangle_c=(k_BT_{\rm ext})^3\ , \tag{3.8}$$
$$\langle K_s^4\rangle_c=\tfrac{15}{4}(k_BT_{\rm ext})^4\ , \tag{3.9}$$

where K_s is the thermostat kinetic energy.

B. Molecular-dynamics simulations

In this section we define the simulation parameters and conditions, and describe the results of the simulations.

TABLE I. The reduced units of *Ne* are compared with the conventional units. m_e is the electron mass and a_0 is the Bohr radius.

Quantity	LJ unit	Conventional unit
Q	1	$1.05\times10^{6}m_e a_0^2$
t	1	2.24×10^{-12} sec
ρ	1	0.050 Å^{-3}
T	1	36.23 K

We then discuss the results by comparing with the generalized Nosé theorem.

In the numerical simulations the reduced units of a LJ system are used. For example, the LJ units of *Ne* are compared with the conventional units in Table I. The equations of motion are solved using the sixth-order Gear predictor-corrector method [1]. To eliminate boundary effects a periodic boundary condition is adapted, and to avoid self-interactions due to the long-range interaction, the LJ potential is cut at r_c ($r_c=2.5$). To compensate the cutoff effect, a long-range correction is made by adding the average of the interaction beyond r_c. The precision of the calculation is monitored by preserving the total energy of the extended system within 0.2% drift during the whole simulations (-0.04% drift for nonzero total momentum, and -0.16% drift for zero total momentum).

To obtain a fast convergence of the moments, a small (32-particle) LJ system is chosen for the simulations. The initial configuration of the simulations is a fcc lattice structure, and the initial velocities are randomly assigned with a given mean value determined by $T_{\rm ext}$. For the case of zero total momentum, the initial velocities are corrected to give a zero sum. On the other hand, for the case of nonzero total momentum, a certain amount of c.m. velocity is added to the initial velocities. The initial values of thermostat and thermostat velocity are chosen to be 1 for all simulations.

In the simulations, the thermostat effective mass Q is chosen to be 1, which gives a fast convergence for the liquid phase ($T_{\rm ext}=1.5$, $\rho=0.8$) of the simulations. Simulations are done with 10^6 time steps for a liquid

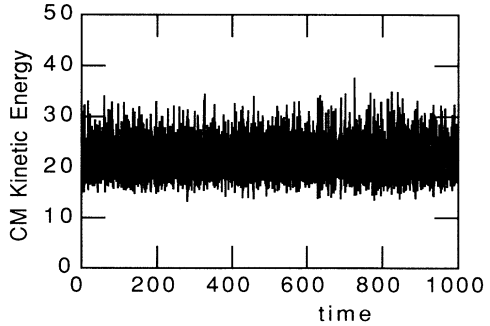

FIG. 2. c.m. kinetic energy K_0/s^2 as a function of time for the extended LJ fluid ($T_{\rm ext}=1.5$, $\rho=0.8$) with nonzero total momentum and thermostat effective mass $Q=1$. The time step is $\Delta t=0.001$, and the total number of time steps is 10^6. Reduced LJ units are used for the energy and the time.

TABLE II. Four moments of the instantaneous temperature of the LJ system, and four moments of the kinetic energy of s are compared with the predicted values of the canonical ensemble. The results are for simulation in the fluid phase ($T_{\rm ext}=1.5$, $\rho=0.8$) of the LJ system with $|\mathbf{P}_0|\neq\mathbf{0}$. The number of time steps is 10^6 and $Q=1$.

	Simulation	Canonical-ensemble value
$\langle T\rangle$	1.504 94	1.5
$\langle T^2\rangle_c$	0.033 64	0.048 39
$\langle T^3\rangle_c$	0.001 41	0.003 12
$\langle T^4\rangle_c$	0.003 44	0.007 22
$\langle K_s\rangle$	0.519 99	0.75
$\langle K_s^2\rangle_c$	0.540 88	1.125
$\langle K_s^3\rangle_c$	1.123 09	3.375
$\langle K_s^4\rangle_c$	4.351 28	18.984

phase ($T_{\rm ext}=1.5$, $\rho=0.8$) for both zero and nonzero total momentum. The total virtual momentum is found to be constant with 5–6 significant figures.

The results of the simulation for nonzero total momentum are shown in Figs. 2–4. Figure 2 shows the c.m. kinetic energy K_0/s^2 as a function of time. Figure 3 shows the average temperature and the average thermostat kinetic energy, and Fig. 4 shows the second moments of temperature and thermostat kinetic energy. The final values of the average moments are summarized in Table II. For this simulation, the c.m. kinetic energy is very large ($\sim 25T_{\rm ext}$), and clearly both the averages and the second moments do *not* converge to the canonical-

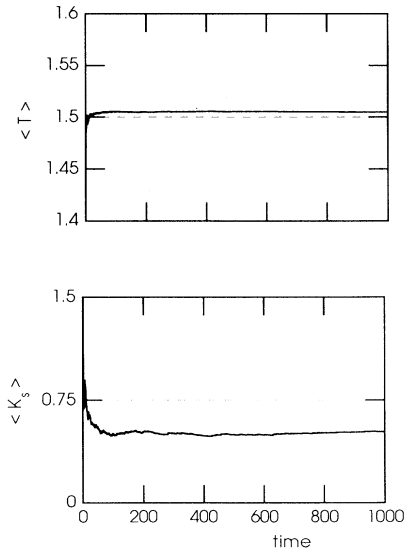

FIG. 3. Average temperature and average thermostat kinetic energy for the extended LJ fluid ($T_{\rm ext}=1.5$, $\rho=0.8$) with nonzero total momentum. The thermostat effective mass is $Q=1$, the time step is $\Delta t=0.001$, and the total number of time steps is 10^6. T is the instantaneous temperature of the LJ system, and K_s is the thermostat kinetic energy. Horizontal dashed lines are the theoretical values of the canonical ensemble. Reduced LJ units are used for the temperature and the time.

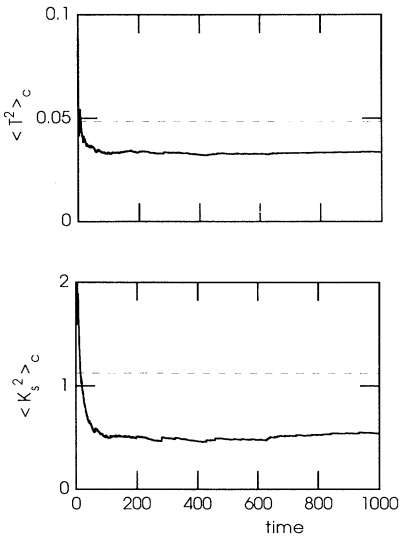

FIG. 4. The second moment of temperature fluctuations and the second-moment thermostat kinetic-energy fluctuation for the extended LJ fluid ($T_{ext}=1.5$, $\rho=0.8$) with nonzero total momentum. The thermostat effective mass is $Q=1$, the time step is $\Delta t=0.001$, and the total number of time steps is 10^6. Horizontal dashed lines are the theoretical values of the canonical ensemble. Reduced LJ units are used for the temperature and the time.

ensemble values shown as dotted lines.

The results of simulations for zero total momentum are shown in Figs. 5–7. Each component of the total momentum is smaller than 10^{-5} during the whole simula-

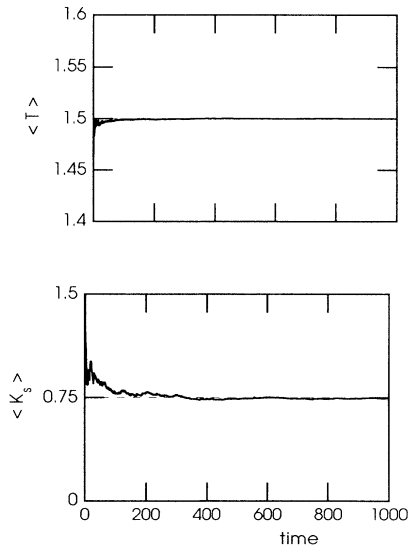

FIG. 5. Average temperature and average thermostat kinetic energy for the extended LJ fluid ($T_{ext}=1.5$, $\rho=0.8$) with zero total momentum. The thermostat effective mass is $Q=1$, the time step is $\Delta t=0.001$, and the total number of time steps is 10^6. Horizontal dashed lines are the theoretical values of the canonical ensemble. Reduced LJ units are used for the temperature and the time.

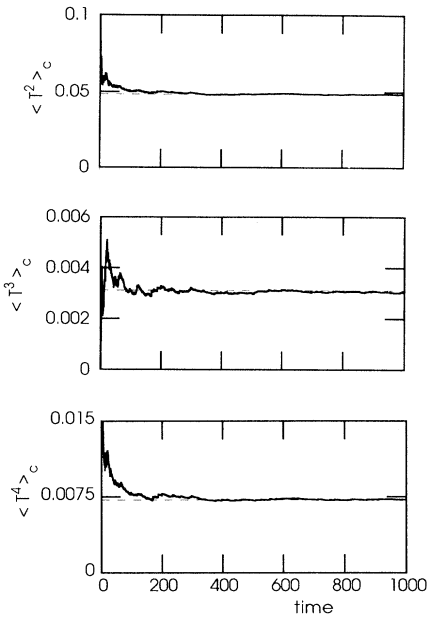

FIG. 6. The second, third, and fourth moments of the temperature fluctuations for the extended LJ fluid ($T_{ext}=1.5$, $\rho=0.8$) with zero total momentum. The thermostat effective mass is $Q=1$, the time step is $\Delta t=0.001$, and the total number of time steps is 10^6. T is the instantaneous temperature for the LJ system, and K_s is the thermostat kinetic energy. Horizontal dashed lines are the theoretical values of the canonical ensemble. Reduced LJ units are used for the temperature and the time.

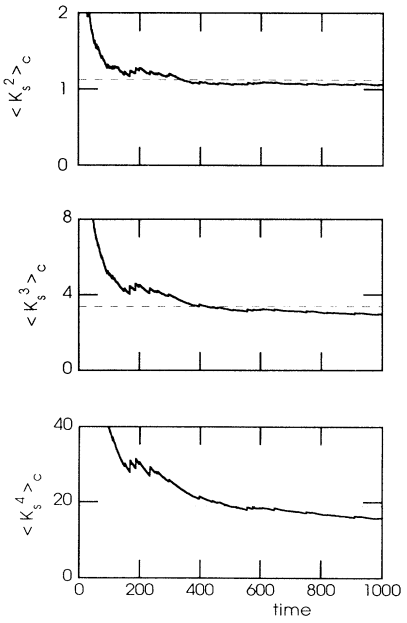

FIG. 7. The second, third, and fourth moments of the thermostat kinetic-energy fluctuations for the extended LJ fluid ($T_{ext}=1.5$, $\rho=0.8$) with zero total momentum. The thermostat effective mass is $Q=1$, the time step is $\Delta t=0.001$, and the total number of time steps is 10^6. Horizontal dashed lines are the theoretical values of the canonical ensemble. Reduced LJ units are used for the temperature and the time.

TABLE III. Four moments of the instantaneous temperature of the LJ system, and four moments of the kinetic energy of s are compared with the predicted values of the canonical ensemble. The results are for simulation in the fluid phase ($T_{\text{ext}}=1.5$, $\rho=0.8$) of the LJ system with $\mathbf{P}_0=\mathbf{0}$. The number of time steps is 10^6 and $Q=1$.

	Simulation	Theory	Error	Corresponding $T_{\text{ext}}^{\text{calc}}$
$\langle T\rangle$	1.500 09	1.5	0.01%	1.500 09
$\langle T^2\rangle_c$	0.048 58	0.048 39	0.39%	1.502 99
$\langle T^3\rangle_c$	0.003 04	0.003 12	−2.56%	1.486 80
$\langle T^4\rangle_c$	0.007 23	0.007 22	0.14%	1.495 06
$\langle K_s\rangle$	0.744 67	0.75	−0.71%	1.489 34
$\langle K_s^2\rangle_c$	1.061 67	1.125	−5.63%	1.457 17
$\langle K_s^3\rangle_c$	2.966 59	3.375	−12.1%	1.436 88
$\langle K_s^4\rangle_c$	15.801 6	18.984	−16.8%	1.432 74

tion. Figure 5 shows that the average temperature and the average thermostat kinetic energy are quite well converged to the canonical-ensemble values. Figure 6 shows that the higher moments of temperature are also very well converged to the canonical-ensemble values. The higher moments of K_s in Fig. 7 show a slower but a reasonable convergence to the canonical-ensemble values. The final values of the average moments are summarized in Table III.

Therefore the simulation with $\mathbf{P}_0\neq\mathbf{0}$ does not produce a canonical ensemble whereas the simulation with $\mathbf{P}_0=\mathbf{0}$ produces a canonical ensemble. Consequently, both simulations of the LJ potential system with zero and nonzero total momentum satisfy the generalized Nosé theorem.

Simulations are also performed with different values of c.m. kinetic energy. For a small c.m. kinetic energy ($\langle K_0/s^2\rangle \leq T_{\text{ext}}$) the results are found to be quite similar to those of zero total momentum. This fact suggests that quite a good approximate canonical ensemble can be generated with nonzero total momentum even if the total momentum is on the order of the external temperature. However, as the c.m. kinetic energy increases ($\langle K_0/s^2\rangle \gg T_{\text{ext}}$), the deviation from the canonical-ensemble values becomes large. These facts guarantee the *numerical stability* of generating a canonical ensemble by ESM in practical applications where computational errors inevitably introduce a small nonzero total momentum. This numerical stability is further discussed in Sec. IV.

IV. PRACTICAL CONSIDERATIONS

In this section we discuss the differences between the Nosé theorem and the generalized Nosé theorem from a practical viewpoint. We discuss three separate topics. The first is the new mass spectrum λ_i of the resulting Hamiltonian satisfying a canonical ensemble. The second is the effect of nonzero total momentum on changing the average moments of temperature and thermostat kinetic energy from canonical-ensemble values. The third is the effect of changing the number of degrees of freedom from $3N$ to $3N-3$ on the interpretation of numerical simulations.

First, in the proof of the generalized Nosé theorem one begins with a physical Hamiltonian with mass spectrum $\{m_i\}$, $i=1,\ldots,N$ and obtains the final Hamiltonian with mass spectrum $\{\lambda_i\}$, $i=1,\ldots,N-1$. In general, the new masses are different from the original masses. For the special case of N identical original masses ($m_i=m$) one finds a final mass spectrum: $\lambda_i=m$ for $i=1,\ldots,N-2$ and $\lambda_{N-1}=m/N$. This new mass spectrum will introduce, in principle, an error in calculations of the dynamical properties. Of course, the conventional MD introduces the same error [11], and as N becomes large, the contribution of the light mass becomes unimportant in practical considerations. As far as thermodynamic averages are concerned, the difference of mass spectra is always irrelevant because of the equipartition theorem. The only significant change relevant to the thermodynamic averages is the reduction of the number of degrees of freedom from $3N$ to $3N-3$.

Second, if $\mathbf{P}_0\neq 0$, then the physical system does not satisfy a canonical ensemble, as we have shown in Sec. II. However, if $|\mathbf{P}_0|$ is small, one can make the following approximations. For small $|\mathbf{P}_0|$, s_1 is very small so that $s_1^{3N-3} \ll s_2^{3N-3}$. Hence one can neglect the first integral containing s_1 in the partition function (2.13). The remaining integral containing s_2 can be approximated as follows:

$$|-K_0/s_2^3+gk_BT_{\text{ext}}/s_2|\approx|gk_BT_{\text{ext}}/s_2|\ , \tag{4.1}$$

since $K_0/s_2^2 \ll gk_BT_{\text{ext}}$ for small $|\mathbf{P}_0|$. After these two approximations, the partition function reduces to the partition function of zero total momentum. The correction is $O(K_0/gk_BT_{\text{ext}})$, and this explains why one can still get good average moments for a small nonzero total momentum as discussed in Sec. III.

Third, if one ignores the momentum conservation entirely as is typically done (i.e., one uses the Nosé theorem to interpret a numerical simulation), then one sets $g=3N+1$ instead of $g=3N-2$, and defines the instantaneous temperature as $T=2K/(3Nk_B)$ rather than Eq. (3.1). Since the Nosé theorem is not strictly valid, one introduces a systematic error in the interpretation of numerical simulations as shown in the following.

In a simulation, one compares the average moments of temperature with those of T_{ext} (3.2)–(3.5), but the value of T_{ext} is defined only as a portion of the coefficient of the thermostat potential

$$gT_{\text{ext}}k_B\ln(s)\ . \tag{4.2}$$

Therefore, when one uses $g=3N+1$ and T_{ext}, it is equivalent to using the correct $g'=3N-2$ with the actual externally set temperature being

$$T'_{\text{ext}}=\frac{g}{g'}T_{\text{ext}}=\frac{3N+1}{3N-2}T_{\text{ext}}\ . \tag{4.3}$$

For a 32-particle system, T'_{ext} is 3.2% larger than T_{ext}. This difference could introduce a significant error in many practical applications. For example, one can obtain a wrong melting temperature by using this interpretation. This error becomes large for a small system so that one should be careful when applying the ESM to

small clusters.

Finally, we note that this error in actual external temperature, although definitely present in a simulation where $g=3N+1$, will not be detected if one simply compares $\langle T=2K/(3Nk_B)\rangle$ with T_{ext}. To see this recall that the actual instantaneous temperature T' is given by Eq. (3.1) so that

$$T'=\frac{3N}{3N-3}T \ . \tag{4.4}$$

According to the generalized Nosé theorem, one must have

$$\langle T'\rangle = T'_{\text{exp}} \ . \tag{4.5}$$

Using (4.3)–(4.5) one then obtains

$$\langle T\rangle = \frac{(3N-3)(3N+1)}{3N(3N-2)}T_{\text{ext}} = \left[1-\frac{3}{3N(3N-2)}\right]T_{\text{ext}} \ . \tag{4.6}$$

This relation means that the errors in T_{ext} and T cancel systematically. For the 32-particle LJ system, the difference between $\langle T\rangle$ and T_{ext} is only 0.03%. We emphasize, however, that both T_{ext} and $\langle T\rangle$ are off by about 3% from the correct value T'_{ext}.

Therefore the use of the Nosé theorem instead of the generalized Nosé theorem in the interpretation of numerical simulations will lead to a systematic error which cannot be detected by a simple "self-consistency" check of comparing $\langle T\rangle$ and T_{ext}. Of course, since the actual error in T_{ext} scales as $O(1/N)$, this error will be important only for systems with a small number of particles.

V. CONCLUSIONS

The Nosé theorem is correct when only the total energy of the system is conserved. In practical applications, the total virtual momentum is also conserved, and therefore the Nosé theorem is no longer strictly valid. Inclusion of the conservation of the total virtual momentum in the original argument of Nosé leads to a generalized Nosé theorem that is valid in practical applications.

The generalized Nosé theorem is proved analytically. As a consequence of the generalized Nosé theorem, if the ES is ergodic and if the total virtual momentum of the N-particle system is zero, then the ESM yields a canonical ensemble for an $(N-1)$-particle system with a different mass spectrum. The consequences of a different mass spectrum are irrelevant to thermodynamic averages, but relevant to the dynamical properties and relaxation times of the system.

The effect of nonzero total momentum is of order K_0/gk_BT_{ext} for small $|\mathbf{P}_0|$. This fact provides a numerical stability of generating a canonical ensemble in practical situations where small nonzero $|\mathbf{P}_0|$ is introduced by computation errors.

Numerical simulations are performed and tested against the generalized Nosé theorem. The simulations are found to satisfy the generalized Nosé theorem and the numerical stability is obtained as expected from the theory.

Finally, in some practical applications, it may be more convenient not to explicitly constrain the total momentum to be zero, but rather transform the physical Hamiltonian to the c.m. coordinate system and *then* couple the Nosé thermostat *only* to the c.m. momenta. In this case one obtains the extended-system Hamiltonian,

$$H'_{\text{ES}}(\mathbf{r}_i,\mathbf{p}_i,s,P_s)=\sum_{i=1}^{N}\frac{\mathbf{p}_i^2}{2m_is^2}+\left[1-\frac{1}{s^2}\right]\frac{\left[\sum_{i=1}^{N}\mathbf{p}_i\right]^2}{2M} +\phi(\{\mathbf{r}_i\})+\frac{P_s^2}{2Q}+gk_BT_{\text{ext}}\ln(s) \ , \tag{5.1}$$

and the following equations of motion:

$$\frac{d^2\mathbf{r}_i}{dt^2}=-\frac{1}{ms^2}\nabla_i\phi-\frac{2}{s}\frac{ds}{dt}\left[\frac{d\mathbf{r}_i}{dt}-\frac{\mathbf{P}_0}{M}\right] , \tag{5.2}$$

$$\frac{d^2s}{dt^2}=\frac{1}{Q}\sum_{i=1}^{N}sm\left[\left[\frac{d\mathbf{r}_i}{dt}\right]^2-\left[\frac{\mathbf{P}_0}{M}\right]^2\right]-\frac{gk_BT_{\text{ext}}}{Q}\frac{1}{s} \ . \tag{5.3}$$

ACKNOWLEDGMENTS

This work was supported in part by U.S. AFOSR Contract No. 87-0098, ONR Contract No. N00014-86-K-0158, NSF Grant No. DMR 90-15222, and the Welch Foundation.

[1] M. P. Allen and D. J. Tildesley, *Computer Simulation of Liquids* (Clarendon, New York, 1987).
[2] Duane C. Wallace and Galen K. Straub, Phys. Rev. A **27**, 2201 (1983).
[3] Even though Newton's equations also satisfy the conservation of the total angular momentum, periodic boundary conditions destroy the conservation of the total angular momentum.
[4] H. C. Anderson, J. Chem. Phys. **72**, 2384 (1980).
[5] M. Parrinello and A. Rahman, J. Appl. Phys. **52**, 7182 (1981).
[6] S. Nosé, J. Chem. Phys. **81**, 511 (1984).
[7] S. Nosé, Mol. Phys. **52**, 255 (1984).
[8] S. Nosé, Prog. Theor. Phys. Suppl. **103**, 1 (1991).
[9] K. Cho and J. D. Joannopoulos, Phys. Rev. A **45**, 7089 (1992).
[10] The virtual variable formalism (Hamiltonian formalism) and other formalisms are reviewed in [9].
[11] One can prove a similar theorem for the conventional MD starting from a partition function similar to Eq. (2.1) with both energy conservation and momentum conservation δ functions of a physical system. For this case, however, the integration of the momentum δ function leads to the microcanonical ensemble of the $(N-1)$-particle system with the mass spectrum $\{\lambda_i\}$ whether $\mathbf{P}_0=\mathbf{0}$ or not.